Science of the Total Environment 685 (2019) 1107–1115

Contents lists available at ScienceDirect

Science of the Total Environment

journal homepage: www.elsevier.com/locate/scitotenv

Molecular characterization of particulate organic matter in full scale anaerobic digesters: An NMR spectroscopy study

Sepehr Shakeri Yekta [a,*], Mattias Hedenström [b], Bo H. Svensson [a], Ingrid Sundgren [a], Mårten Dario [a], Alex Enrich-Prast [a], Norbert Hertkorn [c], Annika Björn [a]

[a] Department of Thematic Studies-Environmental Change and Biogas Research Center, Linköping University, 581 83 Linköping, Sweden
[b] Department of Chemistry, Umeå University, 901 87 Umeå, Sweden
[c] Helmholtz Center Munich, German Research Center for Environmental Health, Research Unit Analytical Biogeochemistry, 85764 Neuherberg, Germany

HIGHLIGHTS

- Structural changes in POM of food and agricultural wastes upon AD were assessed.
- CP-MAS and HSQC NMR characteristics of substrate and digestate POM were compared.
- Labile POM resembles aliphatic lipid structures and starch-like carbohydrates.
- Residual POM resembles protein, lignin, and cellulose-like structures.

GRAPHICAL ABSTRACT

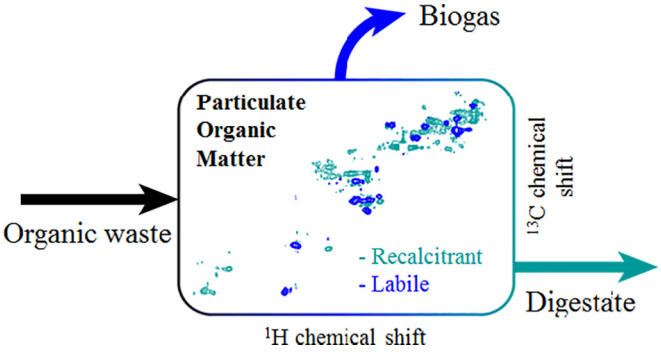

ARTICLE INFO

Article history:
Received 29 January 2019
Received in revised form 4 June 2019
Accepted 17 June 2019
Available online 18 June 2019

Editor: Paola Verlicchi

Keywords:
Anaerobic digestion
Food waste
Agricultural waste
Organic matter
NMR
Digestate

ABSTRACT

This study assesses the molecular characteristics of particulate organic matter (POM) in agricultural and food waste digesters and elucidates the molecular properties of the recalcitrant POM fraction, which remains in the digestate after AD process. Molecular properties of POM in influent (substrate) and effluent (digestate) of seven full-scale AD plants (three agricultural waste and four food waste digesters) were characterized and compared using solid-state ^{13}C cross-polarization magic angle spinning (CP-MAS) and solution-state ^{1}H,^{13}C heteronuclear single-quantum coherence (HSQC) nuclear magnetic resonance (NMR) spectroscopy. Comparison of the POM structural compositions of substrate and digestate from each AD plant revealed an enrichment of protein structures relative to the carbohydrates in most cases, implying a preferential degradation of the carbohydrates over proteins and/or increase of microbial biomass upon AD of agricultural and food wastes. Distinctive molecular structures of labile and recalcitrant fractions of POM, subjected to AD, were identified by comparing the NMR spectra of all substrate and digestate POM. Accordingly, the labile POM fraction in food and agricultural solid wastes is characterized by structural entities of lipids and starch-like carbohydrates, whereas recalcitrant POM structures resemble alkyl and aromatic subunits of amino acids, lignin, and polysaccharides with β-glycosidic linkages. This information serves as a basis to further explore optimization approaches for improving AD of the underutilized POM and the fate of organic matter in digestate-amended arable lands.

* Corresponding author.
E-mail address: sepehr.shakeri.yekta@liu.se (S. Shakeri Yekta).

https://doi.org/10.1016/j.scitotenv.2019.06.264

1. Introduction

Anaerobic digestion (AD) is widely recognized as a promising technology for nutrient and energy recovery from various organic solid wastes, including food and agricultural wastes (Ma et al., 2018). The process involves microbial hydrolysis and solubilization of particulate organic matter (POM), followed by a sequential conversion of the solubilized organic molecules into methane and carbon dioxide (i.e. biogas) via fermentation, acetogenesis and methanogenesis (Schnürer, 2016). Efficiency of the organic matter degradation and biogas production primarily depends on characteristics of the organic substrate, of which resistance or reactivity of POM towards the hydrolysis regulates the degree and kinetics of POM solubilization as the initial reaction for organic matter conversion to biogas (Pavlostathis and Giraldo-Gomez, 1991; Vavilin et al., 2008). In addition, residues of the AD processes, so called digestate, are rich in phosphorus and nitrogen, which has motivated a widespread use of the digestates in agricultural practices as sustainable substitutes for mineral fertilizers (Möller and Müller, 2012). The POM characteristics of the digestate play an important role in the fate of organic matter in agricultural soils, to which digestates are applied as fertilizers. In this context, elucidating the POM characteristics in substrates and digestates of AD processes is fundamental for assessing organic matter conversion processes in anaerobic digesters and in digestate-amended soils.

Organic matter characterization of waste materials is mainly limited to quantification of the bulk proxies such as chemical oxygen demand, biological oxygen demand, and volatile solids or lumped biochemical groups such as total proteins and carbohydrates (Jimenez et al., 2013; Le and Stuckey, 2016). However, the need for optimization of industrial-scale AD processes together with the growing interest for application of digestate as biofertilizer motivate a molecular-level understanding of organic wastes characteristics in order to deal with the diverse nature of wastes from various sources (Hagos et al., 2017). Molecular-level properties of organic matter in anaerobic digesters have been investigated in a few studies, e.g. Shakeri Yekta et al. (2012), Tambone et al. (2013), Provenzano et al. (2014), and Qu et al. (2017), yet such information on POM properties as the primary regulator of organic matter conversion in AD processes is scarce. Therefore, we conducted a detailed study to characterize the molecular structures of POM in influent substrates and effluent digestates of full-scale anaerobic digesters. The study aims to characterize the POM in agricultural and food waste digesters and elucidate the molecular properties of the recalcitrant POM fraction, which remains in the digestate after the AD process.

To characterize the molecular structures of POM, we utilized solid-state ^{13}C cross-polarization magic angle spinning (CP-MAS) and solution-state two-dimensional $^{1}H,^{13}C$ heteronuclear single-quantum coherence (HSQC) nuclear magnetic resonance (NMR) spectroscopy. The ^{13}C CP-MAS NMR method was chosen due to its ability to determine distribution of ^{13}C among major categories of organic molecules without the need of solvent extraction. Solution-state HSQC NMR spectroscopy enables substantially higher resolution and molecular-level assignments of fundamental structural units, not attainable by one dimensional NMR techniques (Hertkorn et al., 2002; Simpson et al., 2011). The novel information provided in the present study allows elucidating molecular structures of labile and recalcitrant POM fractions. This fundamental information serves to further explore potential optimization approaches for improving degradability of the underutilized POM for biogas production and the fate of organic matter in soil, to which the digestate is applied as a biofertilizer.

2. Material and methods

2.1. Sample sources

Organic waste (substrate) and digestate samples were collected from full-scale AD plants in Sweden, including three agricultural waste digesters (CDAW1, CDAW2, and CDAW3) and four food waste digesters (CDFW1, CDFW2, CDFW3, and CDFW4). Sampling points at each plant were substrate-storage units, digester outlets and, if available, post-digester outlets. For AD plants with multiple substrate-storage units, separate substrate samples were collected in order to represent a broad range of organic waste types in the analysis. The procedures for sample collection were chosen in communication with the AD plant operators at each site and followed their routine sampling approaches for regular process monitoring and effluent characterization to ensure representativeness of the samples based on specifications of each operational unit. The CDAW1 and CDAW2 received residual products from agricultural activities such as starch, cereals and silage, whereas the major fraction of the CDAW3 substrate consisted of manure. Substrates of CDFW1 and CDFW2 included minor fractions of slaughterhouse, pig manure, vegetable and food industry wastes in addition to the municipal food waste. Continuous stirred tank reactor technologies are used for all the AD processes except CDFW4, which is a plug-flow reactor. Details on substrate composition and main operational conditions of the AD processes are shown in Table 1.

2.2. Sample preparation

Removal of paramagnetic mineral species from anaerobic digester samples, in particular Fe-containing minerals, is essential prior to NMR spectroscopy, which would otherwise induce signal loss and extensive peak broadening in the NMR spectra (Smernik and Oades, 2000). In a previous study, we demonstrated that pretreatment of the substrate and digestate samples from AD processes by HCl efficiently removed the paramagnetic minerals, yet a partial loss of HCl-soluble organic matter (e.g. readily extractable extracellular polymeric substances) is expected during the sample pretreatment (Shakeri Yekta et al., 2018). Nevertheless, the pretreatment procedure allows for an enhanced NMR-based characterization of organic matter in samples from anaerobic digesters (Shakeri Yekta et al., 2018). To acquire comparable NMR spectra, all samples were treated in a similar way by HCl prior to NMR spectroscopy. Reader is referred to Shakeri Yekta et al. (2018) for detailed information on the HCl pretreatment procedure and its effect on POM characteristics of the anaerobic digester samples. In short, 300–400 mg of freeze-dried samples were weighted in 100-ml glass bottles, to which 25 ml 2 mol l^{-1} HCl was added. The bottles were placed on a magnetic stirrer (300 rpm) and the headspaces were continuously purged with nitrogen gas to flush out potential gases such as hydrogen sulfide, which may evolve after addition of HCl to the samples. After one hour stirring, particles were separated by centrifugation (10,000 ×*g*, 10 min), re-suspended in 50 ml milliQ water to rinse the remaining acid, centrifuged again and the rinse water was decanted. Samples were freeze-dried prior to the NMR spectroscopy analyses. For solid-state ^{13}C CP-MAS NMR spectroscopy, 70 mg of the pretreated samples were packed inside 4 mm ZrO_2 MAS rotors. For solution-state $^{1}H,^{13}C$ HSQC NMR, 200 mg of the samples were ground in a Fritsch Pulverisette 7 premium line planetary ball-mill. The protocol used for grinding consisted of 5 × 10 min milling with 5 min pauses in between to prevent overheating of the samples. After milling, 20 mg of the samples was transferred to 5 mm NMR tubes and 0.6 ml DMSO d_6 (Sigma-Aldrich, USA) was added, followed by mixing using a vortex mixer.

2.3. NMR spectroscopy

^{13}C CP-MAS NMR spectra were acquired on a Bruker 500 MHz Avance III spectrometer operating at a ^{13}C frequency of 125.75 MHz, equipped with a 4 mm MAS probe and a SamplePro sample changer. For each sample, 3500 scans were recorded with a relaxation delay of 1 s, a contact time of 1 ms and a ^{1}H decoupling frequency of 83 kHz during the 23 ms acquisition time. A spin-rate of 10 kHz and a sweep-width of 350 ppm were used for all samples. The $^{1}H,^{13}C$ HSQC NMR spectra were acquired at 25 °C using a Bruker 600 MHz Avance III HD

Table 1
Substrate composition, main operational conditions and sampling points of the full-scale anaerobic digesters.

Site	Substrate composition	OLR[a]	HRT[b]	T[c]	Sampling source (name) [d]
CDAW1	Starch, cereals, forage and corn silage	5.8	55	38	Starch slurry (CDAW1-S1); Cereals (CDAW1-S2); Silage (CDAW1-S3); Digester (CDAW1-D);Post-digester (CDAW1-PD)
CDAW2	Cereals, sugar beets, crop and corn silage	3.1	86	38	Substrate mixture (CDAW2-S); Digester (CDAW2-D); Post-digester (CDAW2-PD)
CDAW3	Pig slurry, chicken and horse manure, deep litter, cereals	3.4	55	38	Manure slurry (CDAW3-S1); Cereals (CDAW3-S2); Digester 1 (CDAW3-D1); Digester 2 (CDAW3-D2)
CDFW1	Municipal food waste, slaughterhouse and food industry wastes	4.2	30	42	Substrate mixture (CDFW1-S); Digester (CDFW1-D); Post-digester (CDFW1-PD)
CDFW2	Municipal food waste, vegetables, food package, slaughterhouse and food industry wastes, pig manure, grease separator sludge	3.0–4.0	25–35	37	Substrate mixture (CDFW2-S); Digester (CDFW2-D); Post-digester (CDFW2-PD)
CDFW3	Municipal food waste	3.1	25–35	38	Substrate mixture (CDFW3-S); Digester (CDFW3-D); Post-digester (CDFW3-PD)
CDFW4	Municipal food waste	4.7	27	55	Substrate mixture (CDFW4-S); Digester (CDFW4-D)

[a] Organic loading rate in g volatile solid per liter per day.
[b] Hydraulic retention time in days.
[c] Operational temperature in °C.
[d] Samples from substrate storage, digester, and post-digester units are indicated by S, D, and PD, respectively.

spectrometer, equipped with a 5 mm BBO cryoprobe with z-gradients and a SampleJet auto-sampler. The spectra were recorded using adiabatic ^{13}C inversion pulses with sweep-widths of 8.14 and 140 ppm in the ^{1}H and ^{13}C dimensions and with a relaxation delay of 2 s, resulting in a total acquisition time of approximately 75 min per sample. For each of the 128 increments in the indirect dimension, 16 scans were recorded. Zero filling in the indirect dimension was applied, resulting in a 1024×512 spectral matrix. A Gaussian window function with a line-broadening of −0.1 Hz for ^{1}H, −1 Hz for ^{13}C, and a GB of 0.001 in both dimensions was applied prior to the Fourier transformation. Spectra were processed by Topspin 3.2 software (Bruker Biospin, Germany).

2.4. NMR data analysis

Principal component analysis (PCA) was carried out in order to investigate variations in the NMR spectral dataset (i.e. signal intensities across the chemical shift dimensions) and to identify signal resonances, which substantially contributed to the observed variations among the NMR spectra (Eriksson et al., 2004). Orthogonal projections to latent structures discriminant analysis (OPLS-DA) was implemented for extracting and comparing latent spectral patterns (Trygg and Wold, 2002), which allows to assess whether there are any systematic variations among the spectra that are explicitly related to the POM origin (i.e. either from the substrate or from the digestate samples). The multivariate statistical analyses were performed on spectral data normalized to a constant sum using Simca 13.0 (Umetrics, Sweden). In case of the ^{1}H,^{13}C HSQC data, an in-house Matlab (Mathworks Inc.) script, available from the authors upon request, was used to import the raw data, reshaping each spectrum into a row vector and normalizing each spectrum (Hedenström et al., 2009). This script was further used to set the intensity of all data-points belonging to the DMSO d_6 peak to zero. For evaluation of the chemical shift regions and peaks within ^{13}C CP-MAS and ^{1}H,^{13}C HSQC NMR spectra, signal assignments were made based on literature data, reference spectra on model compounds and, in some cases, spectral simulation using ACD/Spectrus Processor 2015.2.5 (ACD/Labs, Canada). Spectra were recorded for Peptone, 1-Palmitoyl-2-oleoyl-sn-glycero-3-phosphoglycerol (POPG), microcrystalline cellulose and wheat starch, which served as representative NMR fingerprints of the protein, lipid, and carbohydrate fractions present in the complex organic matrices of the POM.

2.5. Chemical analysis

The overall chemical properties of the samples including total solid (TS), volatile solid (VS), Kjeldahl N, ammonium N, protein and carbohydrate (i.e. xylose, mannose, glucose, galactose, and arabinose) contents were determined by Eurofins Environment Testing Sweden AB (Lidköping, Sweden). Total solid and VS contents were determined according to the Swedish standard method SS028311. Kjeldahl and ammonium N were determined according to the standard methods SS-EN 13342 and 4500, respectively (www.standardmethods.org). Total protein concentrations were roughly estimated as differences between concentration of Kjeldahl and ammonium N, multiplied by a conversion factor of 6.25 for crude proteins (Official Methods of Analysis of AOAC International). Concentration of carbohydrate monomeric units was determined according to SCAN-CM 71:09 (Scandinavian pulp, paper and board testing committee, Stockholm, 2009). The C and N contents of milled POM samples were determined by an elemental analyzer according to the manufacturer's instruction (Series II CHNS/O analyzer, Perkin Elmer, USA). Analyses of elemental C and N contents in multiple reference sludge samples (CRM029050, RTC, USA) had a relative standard deviation of 3% and 5% of the certified values, respectively, which were considered as analytical uncertainties.

3. Results and discussion

3.1. ^{13}C CP-MAS NMR analysis of digestate POM

Solid-state ^{13}C NMR spectra of molecularly heterogeneous organic samples, such as digestate POM, display resonances over a wide range of chemical shifts, which can be divided into the regions assignable to alkyl (δ_C: 0–47 ppm), O-alkyl (δ_C: 47–90 ppm), anomeric (δ_C: 90–108 ppm), aromatic (δ_C: 108–145 ppm), O,N-substituted aromatic (δ_C: 145–167 ppm), and carbonyl groups (δ_C: 167–220 ppm) (Hertkorn et al., 2002). Principal component analysis was performed to assess variations among the ^{13}C CP-MAS NMR spectra. The first and second principal components explained 97% of the variations and revealed systematic differences in the spectral data (Fig. 1). Samples from agricultural waste digesters (CDAW1, CDAW2, and CDAW3) positioned on the right hand side of the scores plot along the first principal component, whereas the food waste digesters (CDFW1, CDFW2, and CDFW3) positioned on the left (Fig. 1A). The CDFW4 samples were clustered separately at the top of the scores plot along the second principal component (Fig. 1A). These observations imply that the substrate source is likely the major contributor to the spectral variations and separation of the samples in the scores plot (cf. Fig. 1A).

Evaluation of PCA loading plots revealed that the spectral variations along the first principal component are partly due to different intensities of O-alkyl and anomeric C resonances, which were higher in digestate POM from agricultural waste digesters compared to the food waste digesters, with the exception of CDFW4 (Fig. 1B). The O-alkyl and anomeric C regions contain prominent resonances from carbohydrates as well as potential overlap of signals from CH and CH_2 in glycerol (δ_C: 50–80 ppm), N-alkyl C in proteins (δ_C: 45–60 ppm), methoxyl C in

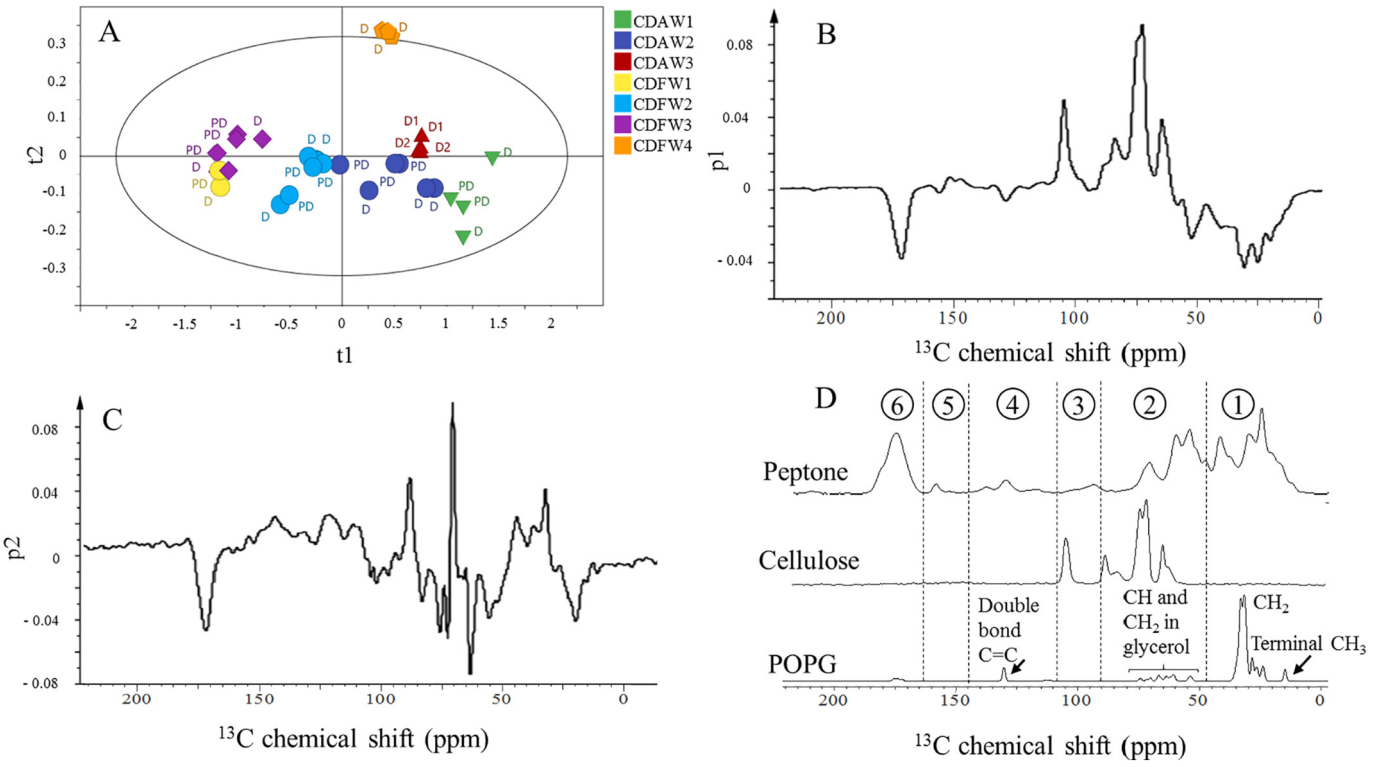

Fig. 1. A) Principal component analysis (PCA) scores plot of ^{13}C CP-MAS NMR signal intensities from digestate POM. Samples from digester and post-digester units are indicated by D and PD, respectively. Detailed information on sample sources are presented in Table 1 B) First loading plot, showing ^{13}C NMR signals that contributed to variation in spectral data along the first principal component (x-axis) of the scores plot. Positive values represent higher intensities of the peaks on the right hand side of the scores plot and negative values represent peaks with lower intensities on the right side of the scores plot. C) Second loading plot, showing the ^{13}C NMR signals which contributed to variation along the second principal component (y-axis) of the scores plot. D) Spectra of POPG, cellulose, and peptone as examples of ^{13}C CP-MAS NMR spectra of lipids, carbohydrates and proteins. Dashed lines mark spectral regions attributed to 1) alkyl, 2) O-alkyl, 3) anomeric 4) aromatic, 5) O,N-substituted aromatic, and 6) carbonyl C. Specific assignments in D are indicated for POPG based on simulation of ^{13}C chemical shifts (see Fig. S1 for details).

lignin (δ_C: 55 ppm), and high field aromatic C signals (Fig. 1D) (Hertkorn et al., 2002; Simpson et al., 2007). We observed that the integrals of O-alkyl and anomeric C in the digestate POM spectra significantly correlated with the measured concentrations of xylose, glucose and arabinose in the samples ($r_{Pearson} = 0.87–0.97$, $p < 0.01$; Fig. S2A). Thus, differences in O-alkyl and anomeric C resonances mainly reflect the varying contents of (hemi)cellulosic carbohydrates in the digestate POM.

Furthermore, variable resonances from alkyl and carbonyl C contributed to the observed variations among the digestate POM spectra (Fig. 1B), with relatively higher intensities in spectra from food waste digesters (CDFW1, CDFW2, and CDFW3). The alkyl C region comprises resonances of aliphatic CH_2 and terminal CH_3 units of lipids and proteins, while carbonyl C signals are mainly related to the presence of proteins as displayed by the spectrum of peptone (Fig. 1D). The integrals of alkyl and carbonyl C in spectra of digestate POM positively correlated to each other and to the N contents of the POM ($r_{Pearson} = 0.97$, $p < 0.01$; Fig. S2B and S2C), further supporting that these resonances originate mainly from proteins. Variations in spectral data represented by the second principal component were relatively small, except for CDFW4 (Fig. 1A). The second loading plot of the PCA showed a complex, irregular pattern, and no detailed interpretation was attempted (Fig. 1C). Nevertheless, we observed a positive correlation between peaks in the alkyl region, which may be interpreted as higher contributions of lipids in the digestate POM from CDFW4. This was also observed in the ^{1}H,^{13}C HSQC NMR spectra as discussed in the following sections.

3.2. Comparison of ^{13}C NMR spectra of substrate and digestate POM

Signal integrals of different ^{13}C chemical shift intervals (cf. Fig. 1D) are presented for all substrate and digestate POM spectra in Table S1. We emphasize that the ^{13}C CP-MAS NMR analysis is inherently non-quantitative, though the integral values of different spectral regions (% of total area) may be used as quantitative proxies for relative C distribution among major structural POM categories in the samples. As a general trend, the O-alkyl C had the highest relative integrals in the POM samples followed by the alkyl C resonances (Table S1). The highest O-alkyl C integrals were observed for CDAW1 substrates (i.e. starch slurry: 60%, cereals: 63%, and silage: 62% of total integrals) and the lowest O-alkyl C integral was observed for digestate from CDFW1 and CDFW3 (33–36% of total integrals). The O-alkyl C integrals were generally lower for the digestate POM compared to the corresponding substrate POM, while alkyl C integral values were higher (Table S1). The alkyl to O-alkyl C ratios, which manifest the relative contents of protein and carbohydrate, were higher in digestate POM compared to the corresponding substrate POM (Table S1), reflecting a decrease in the contents of O-alkyl C relative to alkyl C after anaerobic degradation of organic wastes. This trend is particularly evident for the AD plants, from which a mixture of influent organic wastes could be collected as a single substrate sample (CDFW1, CDFW3, CDFW4, and CDAW2), with the exception of CDFW2 (Table S1). The alkyl to O-alkyl C ratios were disproportional to the C:N ratios, which were mainly lower in the digestate compared to the substrate POM (Fig. S2D). The lower C:N ratios of the anaerobically digested POM indicate a higher N content (e.g. from proteins and microbial biomass) relative to C in the solid phase compared to the substrate, which is likely due to mineralization of the biodegradable organic C during AD.

The ^{13}C NMR characteristics of digestate and substrate POM corroborated the results obtained from quantitative measurements of carbohydrate monomeric units and estimation of total proteins in the samples (Table S2). Protein to carbohydrate ratios were generally higher in digestates compared to their organic waste substrates, similar

to the trend observed for alkyl to O-alkyl C ratios (Table S2). We would like to emphasize that these results do not imply that the proteins accumulated or were not degraded in the digesters, rather their proportion in POM was higher relative to the carbohydrates compared to the substrate. This is in line with previous observations, which suggested a generally higher efficiency and preferential degradation of carbohydrates over proteins under anaerobic conditions (Breure et al., 1986; Giri et al., 2016; Yang et al., 2015). A clear deviation from this trend was observed for samples from the CDFW2 plant, in which the protein to carbohydrate ratio in the substrate was higher than the digestate POM (Table S2). The digestate POM from CDFW2 also contained a higher proportion of O-alkyl C and a lower proportion of alkyl C compared to the corresponding substrate POM as opposed to the other food waste digesters (Table S1). We did not observe any exceptional differences in ^{13}C NMR characteristics of POM in CDFW2 samples (Table S2) and no apparent conclusion can be drawn regarding the potential differences in biodegradability of the carbohydrate fraction in CDFW2 compared to the other digesters based on the NMR spectroscopy data. The substrate POM samples from CDFW2 plant had relatively low C/N ratio (Table S1) and the corresponding digestate samples contained the highest concentration of ammonium-N compared to the other digesters in this study (Table S2). Anaerobic digestion of substrates with low C/N ratios (i.e. N-rich substrates) and potential disturbances of methanogenic activities due to ammonia inhibition is well documented (Chen et al., 2014), yet the mechanism of ammonia effects on hydrolysis of carbohydrates is not well understood. Nevertheless, it has been demonstrated that high ammonia levels may negatively affect the activity and establishment of cellulose-degrading microbial communities, resulting in an inefficient carbohydrate degradation during AD of N-rich substrates (Liu et al., 2017; Sun et al., 2016). Accordingly, a relatively high ammonium/ammonia level in digestate POM from CDFW2 (cf. Table S2) might have contributed to an enrichment of the carbohydrates.

Integrals of aromatic C ranged between 5 and 18% of total integrals (Table S1) and were consistently higher in the digestate POM compared to the corresponding substrate POM, indicating an enrichment of the aromatic structures upon AD of organic wastes (Table S1). Digestate POM samples from CDFW4 (the only thermophilic, plug-flow food waste digester in this study) had the highest relative abundance of aromatic C (18% of total integrals). The anaerobic degradation of aromatic compounds (e.g. phenolic substances) is generally limited under thermophilic conditions, whereas similar compounds may decompose under anaerobic mesophilic conditions (Karlsson et al., 1999; Levén and Schnürer, 2005). Thus, the higher operational temperature of the CDFW4 may have contributed to a more extensive enrichment of the aromatics in the POM of the digestate, in particular compared to the mesophilic AD processes with food waste as their main substrate (Table S1). It should be noted that aromatic C signals at ^{13}C chemical shift range of 108–167 ppm include contributions from overlap of olefinic C, which resonates at ^{13}C chemical shift of ~130 ppm (Fig. 1D). Contribution of the olefinic C to structural composition of POM will be further discussed along with presentation of $^{1}H,^{13}C$ HSQC NMR data.

3.3. $^{1}H,^{13}C$ HSQC NMR analysis of digestate POM

Cross peaks within different chemical shift regions of $^{1}H,^{13}C$ HSQC NMR spectra represent resonances from CH bonds in four main structural groups, typically assigned to aliphatic ($\delta_{H/C}$: 0.4–3.4/5–40 ppm), carbohydrate ($\delta_{H/C}$: 3.0–5.3/50–85 ppm), anomeric ($\delta_{H/C}$: 4.2–5.6/85–105 ppm), and aromatic ($\delta_{H/C}$: 6.0–9.0/105–145 ppm) subunits (Hertkorn et al., 2002; Simpson et al., 2011). Assignments of specific peaks or peak patterns can be corroborated by comparison with spectra acquired from model compounds, literature data, and/or spectral simulation (Kelleher and Simpson, 2006). In the present paper, such assignments are exemplified for lipid-derived cross peaks in Fig. 2A, through a comparison of the simulated and experimental $^{1}H,^{13}C$ HSQC NMR spectra of POPG (Fig. S3). Assignments for major structural units of carbohydrates (i.e. OCH_2, OCH and O_2CH in pyranose ring structures) are shown for spectra of microcrystalline cellulose in Fig. 2B. A general spectral fingerprint for proteins is exemplified for peptone in Fig. 2C and peak assignments are made according to ^{1}H and ^{13}C chemical shifts presented by Hertkorn et al. (2002).

Overall features of the HSQC NMR spectra of the digestate POM were qualitatively similar, containing signals in four main chemical shift regions attributed to aliphatic, carbohydrate, anomeric, and aromatic groups (Fig. S4). Despite the visual similarities, PCA of the spectral data revealed a substantial variation among the digestate POM samples from different sites (Fig. 2D). The first and the second principal components explained 86% of the variations in the spectral data. The feature of the scores plot in Fig. 2D resembles the PCA scores plot obtained based on the solid-state ^{13}C spectral data (cf. Fig. 1A), as both types of NMR experiments share information on ^{13}C resonances of the POM. However, the $^{1}H,^{13}C$ HSQC NMR experiment allows for a more detailed analysis of POM structural composition at molecular level due to its superior resolution. The PCA loading plots in Fig. 2E and F display the CH resonances, which contributed to the variation in the $^{1}H,^{13}C$ HSQC NMR characteristics of the samples from different AD processes. According to the first loading plot (Fig. 2E), two main groups of cross peaks contributed to the spectral variations, including 1) OCH_2, OCH, O_2CH, $C_{aromatic}$-$COOCH_3$ (lignin-derived methoxyl), and CH_3-CO-R (acetyl) cross peaks as well as 2) amino acids resonances (i.e. CH_3, CH_2, CHα and side-chain aromatic CH) together with CH_3 and aliphatic CH_2 cross peaks from lipids. In line with the results of solid-state ^{13}C NMR spectroscopy, carbohydrate-derived resonances had high intensities in HSQC NMR spectra of agricultural waste digesters (CDAW1, CDAW2, and CDAW3), whereas high intensities of the protein- and lipid-derived signals were largely associated with the spectra of digestate POM from food waste digesters (CDFW1, CDFW2, and CDFW3; Fig. 2D).

The digestate POM of CDFW4 encompassed different structural composition compared to the other samples and clustered separately in the scores plot (Fig. 2D). Evaluation of the loadings along the second principal component (Fig. 2F) showed that higher intensities of lipid-derived peaks contributed to a separate clustering of the CDFW4 samples. This included peaks assignable to main-chain CH_2, $CH_2(\alpha)$, CH_2 adjacent to double bonds, CH of double bonds as well as peaks at $\delta_{H/C}$: 3.2–3.7/55–75 ppm, tentatively assigned to glycerol end and/or lipid headgroups. An overall conformity of the solution-state NMR results with the results from the non-destructive solid-state ^{13}C NMR implies that the relative signal intensities in HSQC NMR spectra of DMSO d_6 soluble POM provides reasonable representations of the C distribution among different structural components of the POM.

3.4. Comparison of $^{1}H,^{13}C$ HSQC NMR spectra of substrate and digestate POM

Variations in spectral data from substrate POM showed a pattern similar to the digestate POM, in which the intensities of carbohydrate-derived peaks were relatively high in POM spectra of agricultural wastes, while protein- and lipid-derived cross peaks appeared with high intensities in spectra of food waste samples (data not shown). We performed PCA on all $^{1}H,^{13}C$ HSQC NMR spectra to elucidate any major differences between the chemical composition of substrate and digestate POM. The PCA of combined data did not result in any clear separation between the substrate and digestate spectra, presumably due to large variations in the spectral properties within each sample group. Therefore, we classified the samples into two groups of “substrate” and “digestate” and used OPLS-DA (Fig. 3). This approach gathers variations correlated to a sample class in a single component, allowing to exclude orthogonal variations and to identify even minor differences between the spectra, which is correlated to each sample group (Trygg and Wold, 2002).

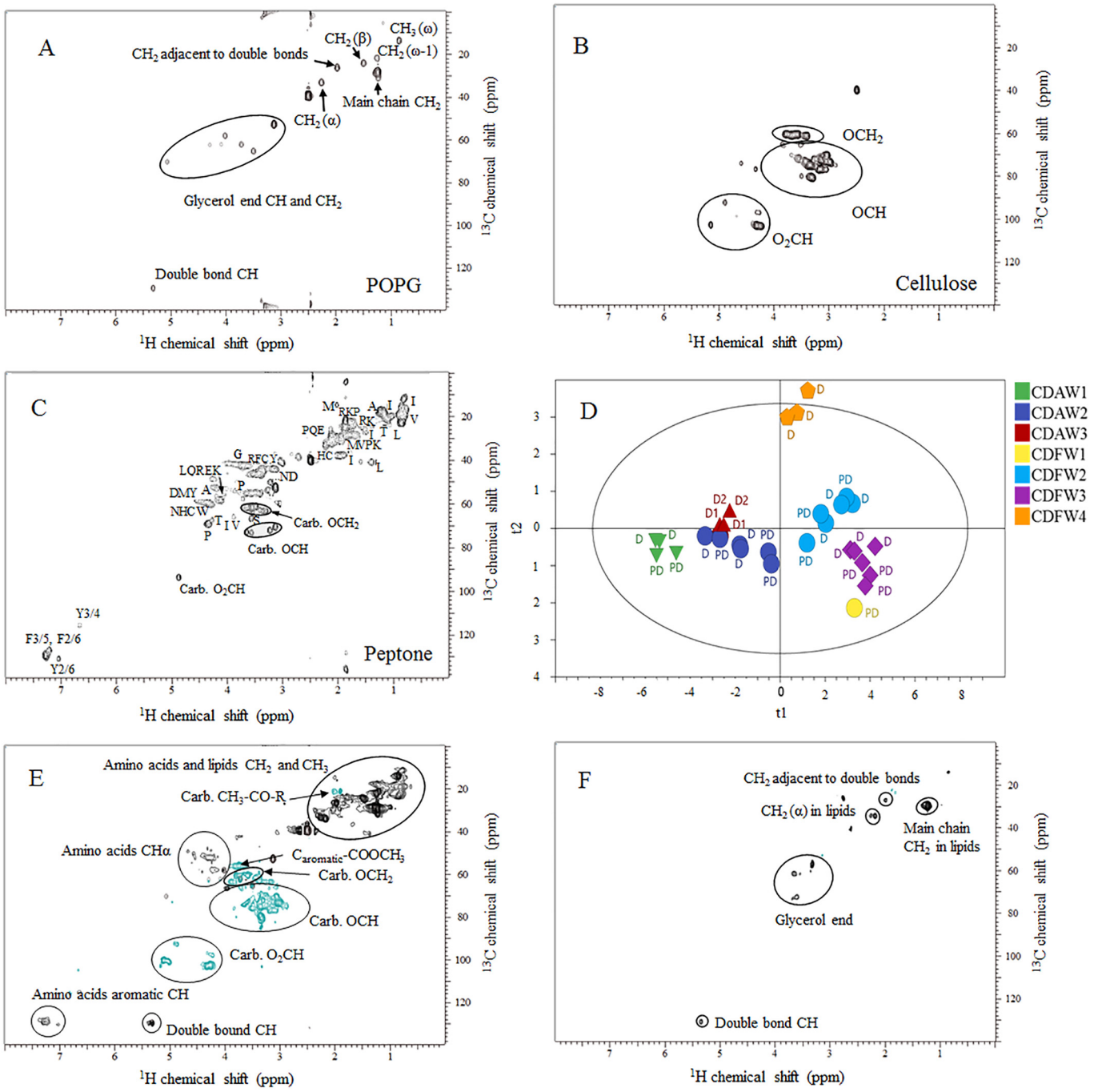

Fig. 2. Spectra acquired from POPG (A), cellulose (B), and peptone (C) as examples for the $^{1}H,^{13}C$ HSQC NMR spectral features of lipids, carbohydrates and proteins, respectively. Specific assignments for POPG are based on comparison of the experimental and simulated spectra (Fig. S3). Tentative assignments of protein cross-peaks are according to ^{1}H and ^{13}C chemical shifts presented by Hertkorn et al. (2002), with letters representing amino acids in open coil proteins following alanine. D) Principal component analysis (PCA) scores plot of $^{1}H,^{13}C$ HSQC NMR spectra of digestate POM. Samples from digester and post-digester units are indicated by D and PD, respectively. Detailed information on sample sources are presented in Table 1 E) First loading plot displaying the peaks responsible for the variation in data along the x-axis of the scores plot. Positive values (black) represent an increase in normalized signal intensities from left to right and negative values (green) represent an increase in signal intensities from right to left along the x-axis of the scores plot. F) Second loading plot, displaying the peaks responsible for the variation in data along the y-axis of the scores plot. (For interpretation of the references to colour in this figure legend, the reader is referred to the web version of this article.)

The OPLS-DA explained 65% of the variation (R^2X) in the spectral data and had a predictive ability of 85% (Q^2Y). The predictive component, t_p, indicated a clear separation of the samples defined as either substrate or digestate (Fig. 3A). The orthogonal component, t_o, reflects spectral differences between the samples within each group. According to the loading spectrum of the OPLS-DA (Fig. 3B), peaks that positively correlated to the substrate POM are lipid-derived $CH_3(\omega)$ at $\delta_{H/C}$:0.9/14.4, main-chain CH_2 at $\delta_{H/C}$:1.3/29.2, $CH_2(\omega\text{-}1)$ at $\delta_{H/C}$:1.3/22.5, CH_2 (β) at $\delta_{H/C}$:1.5/24.8, CH_2 adjacent to double bonds at $\delta_{H/C}$:2.0/27.0, CH_2 (α) at $\delta_{H/C}$:2.2/33.8, and double bonds CH at $\delta_{H/C}$:5.3/129.8. A correlation peak at $\delta_{H/C}$:3.1/53.3 is likely related to the glycerol unit of the lipids, which was also observed in the $^{1}H,^{13}C$ HSQC NMR spectrum of POPG (Fig. S3). Furthermore, carbohydrate peaks of OCH_2 at $\delta_{H/C}$:3.6/60.3, OCH at $\delta_{H/C}$:3.1/69.8, $\delta_{H/C}$:3.3/71.9, $\delta_{H/C}$:3.3/79.3, $\delta_{H/C}$:3.6/71.6, and $\delta_{H/C}$:3.7/72.8 together with O_2CH at $\delta_{H/C}$:5.0/100.4 were positively correlated to substrate POM. These peaks could be attributed to

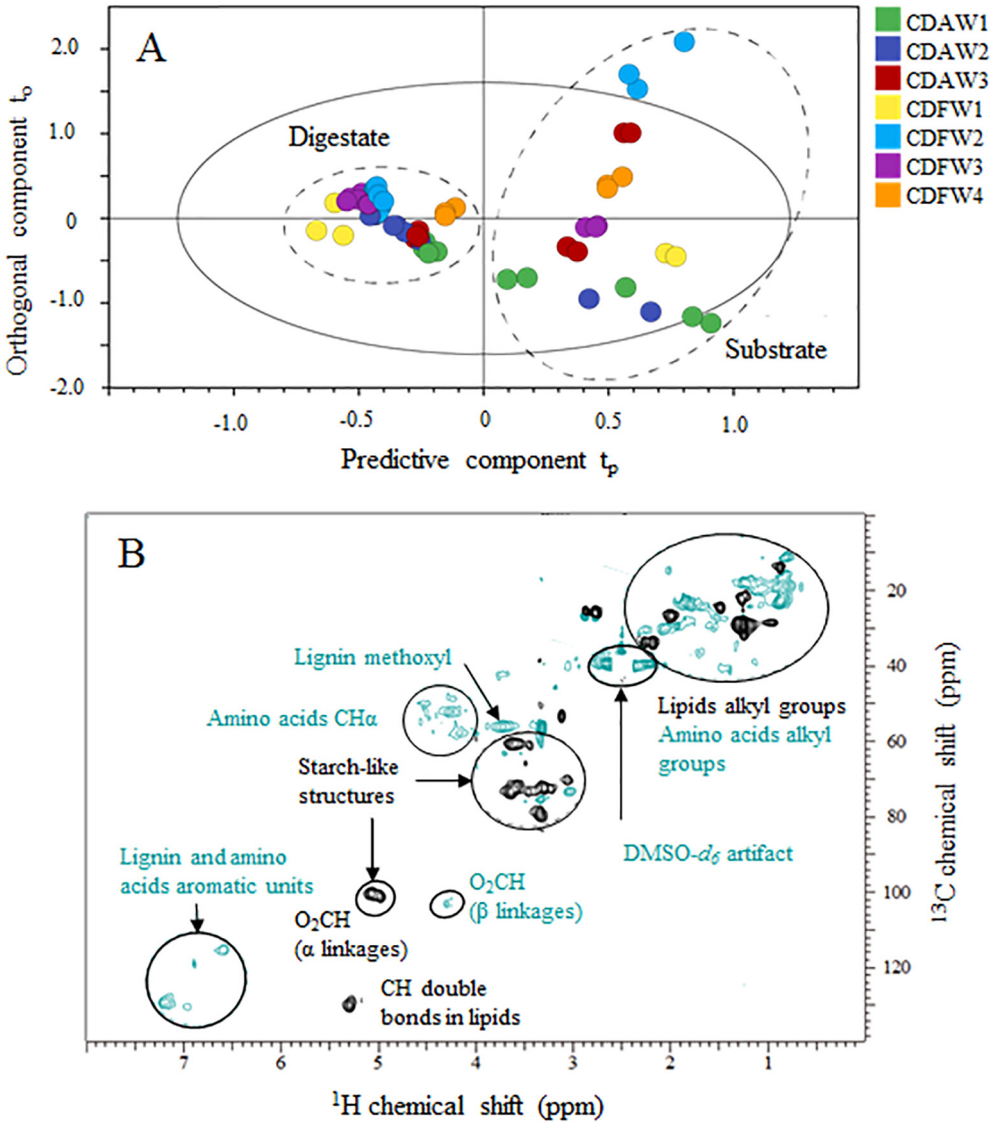

Fig. 3. A) Scores plot from the orthogonal projections to latent structures discriminant analysis (OPLS-DA) of the $^{1}H,^{13}C$ HSQC NMR spectra. The predictive component, t_p, shows separation of the samples based on their classification as either substrate or digestate. The orthogonal component, t_o, reflects spectral differences between AD processes within each substrate and digestate group. B) Loading spectrum showing the spectral differences along the predictive component and the peaks that are positively correlated either to substrate (black) or digestate (green). The overall signal assignments are presented and the reader is referred to Fig. 2 for details on the peak assignments. (For interpretation of the references to colour in this figure legend, the reader is referred to the web version of this article.)

starch-like structures through comparison with a reference spectrum of wheat starch (Fig. S5). Spectra from digestate POM were positively correlated to various protein-derived peaks of aliphatic CH_3, CH_2, CHα and aromatic CH-groups in amino acids and lignin as well as signals related to the methoxyl OCH_3 group of lignin. A cross peak at $\delta_{H/C}$:4.3/102.6 in the anomeric region of the spectra (i.e. carbohydrate O_2CH) was correlated to digestate POM, which may be attributed to cellulose-like polysaccharide structures with β-glycosidic linkages (Soucémarianadin et al., 2017).

The peaks positively correlated with the digestate POM represent the structural features of recalcitrant organic matter, which remained after the AD process. On the contrary, peaks correlated to the substrate POM belong to more labile structural elements, which underwent microbial hydrolysis during AD and consequently, were depleted in the digestate POM. Thus, aliphatic entities of lipid structures and starch-like constituents of carbohydrates characterized the structural composition of labile POM in agricultural and food wastes, subjected to AD. On the other hand, molecular structures of residual and recalcitrant POM bear a resemblance to the molecular structures of proteins and lignin as well as polysaccharides with β-glycosidic linkages.

In agreement with association of the lipid-like structures to the substrate POM, we also observed that the ratios between signal intensities of lipid-derived CH_3 and CH_2 groups were higher in the digestate POM as compared to the substrate POM for all AD plants (Fig. S6). A higher aliphatic CH_3 to CH_2 ratio represents shorter aliphatic chain lengths and/or presence of branched moieties in an organic matrix (Evaristi et al., 2016). Similar observations pointing at the degradation of aliphatic lipid-like structures upon AD has also been reported based on Fourier-transform infrared spectroscopy of organic matter of pig slurry substrate (Marcato et al., 2009). In addition, we observed that ratios between signal intensities of olefinic CH and lipid-derived CH_2 groups were lower in the digestate POM compared to the substrate POM (Fig. S6), indicating lower abundances of the unsaturated bonds in fatty acid fraction of POM. Accordingly, the observed differences in signal intensities of lipid-derived resonances between substrate and

digestate POM reflect the degradation of aliphatic chains and olefinic bonds of the fatty acids during AD of agricultural and food wastes.

4. Conclusions

Characterization of POM molecular structures of the digestate samples from full-scale agricultural and food digesters revealed that the structural composition of the POM differs among different AD processes mainly according to the substrate source. Qualitative and quantitative analyses of POM properties indicated that the carbohydrate fraction of the organic wastes with starch-like structural properties was depleted in the majority of the AD processes, yet cellulose-like structures (characterized by β-glycosidic bonds) were enriched in the digestates, particularly from AD of agricultural wastes. The overall carbohydrate degradation was exceptionally limited in an AD process with a relatively high level of ammonium N, which is in line with previously reported negative effects of ammonium/ammonia on anaerobic degradation of cellulosic substrates. However, further research is required to confirm potential effects of ammonium/ammonia levels in anaerobic digesters on the degree of carbohydrate hydrolysis.

Information provided on molecular structures of the digestate POM provides background for further evaluation of the impact of organic matter in digestate-amended arable lands. Furthermore, this information can serve as a basis for implementing different digestate valorization approaches. For instance, an improved biogas production may be achieved via digestate post-treatment coupled to post-digestion or recirculation of the digestate (Monlau et al., 2015; Sambusiti et al., 2015; Svensson et al., 2018). Indeed, five of the full-scale AD plants in our study have already installed post-digestion units and consider developing methods for digestate post-treatment in order to improve the biogas yield of the post-digesters (personal communications with biogas plant managers). Digestate POM from AD processes with food waste as their major components exhibited high intensities of peaks in the aliphatic and aromatic spectral regions of both the solid-state ^{13}C CPMAS and the solution-state $^{1}H,^{13}C$ HSQC spectra, associated with protein-like substances. Thus, post-treatment approaches may be optimized towards enhancing hydrolysis of the proteinous compounds in the digestates from AD of food waste. Coupling assessments of the effects of post-treatment on structural characteristics of POM to its impact on accessibility of the digestate POM in order to enhance the biogas production from residual organic matter will be the focus of future studies.

Acknowledgements

This work was supported by the Swedish Energy Agency [Grant number: 35624-2], the Swedish Research Council Formas [Grant number: 2016-01054], and the Knut and Alice Wallenberg foundation program NMR for Life (www.nmrforlife.se). The research was conducted within the activities of Biogas Research Center (BRC) hosted by Linköping University, Sweden. Tekniska Verken i Linköping, Scandinavian Biogas Fuels, NSR, Swedish Biogas International, Västblekinge Miljö and Purac are acknowledged for their active contributions to the project. We would like to thank prof. Anna Schnürer for her valuable inputs and discussions within this project.

Appendix A. Supplementary data

Supplementary data to this article can be found online at https://doi.org/10.1016/j.scitotenv.2019.06.264.

References

Breure, A.M., Mooijman, K.A., van Andel, J.G., 1986. Protein degradation in anaerobic digestion: influence of volatile fatty acids and carbohydrates on hydrolysis and acidogenic fermentation of gelatin. Appl. Microbiol. Biotechnol. 24, 426–431.
Chen, J., Ortiz, R., Steele, T., Stuckey, D., 2014. Toxicants inhibiting anaerobic digestion: a review. Biotechnol. Adv. 32, 1523–1534.
Eriksson, L., Antti, H., Gottfries, J., Holmes, E., Johansson, E., Lindgren, F., et al., 2004. Using chemometrics for navigating in the large data sets of genomics, proteomics, and metabonomics (gpm). Anal. Bioanal. Chem. 380, 419–429.
Evaristi, M.F., Caubère, C., Harmancey, R., Desmoulin, F., Peacock, W.F., Berry, M., et al., 2016. Increased mean aliphatic lipid chain length in left ventricular hypertrophy secondary to arterial hypertension: a cross-sectional study. Medicine 95, e4965.
Giri, S.S., Saha, S., Park, S.C., 2016. Comparison of degradation properties of carbohydrate and protein during anaerobic digestion of activated sludge at mesophilic temperature. Int. J. Environ. Waste Manag. 18, 213–225.
Hagos, K., Zong, J., Li, D., Liu, C., Lu, X., 2017. Anaerobic co-digestion process for biogas production: Progress, challenges and perspectives. Renew. Sust. Energ. Rev. 76, 1485–1496.
Hedenström, M., Wiklund-Lindström, S., Öman, T., Lu, F., Gerber, L., Schatz, P., et al., 2009. Identification of lignin and polysaccharide modifications in populus wood by chemometric analysis of 2D NMR spectra from dissolved cell walls. Mol. Plant 2, 933–942.
Hertkorn, N., Permin, A., Perminova, I., Kovalevskii, D., Yudov, M., Petrosyan, V., et al., 2002. Comparative analysis of partial structures of a peat humic and fulvic acid using one- and two-dimensional nuclear magnetic resonance spectroscopy. J. Environ. Qual. 31, 375–387.
Jimenez, J., Vedrenne, F., Denis, C., Mottet, A., Déléris, S., Steyer, J.P., et al., 2013. A statistical comparison of protein and carbohydrate characterisation methodology applied on sewage sludge samples. Water Res. 47, 1751–1762.
Karlsson, A., Ejlertsson, J., Nezirevic, D., Svensson, B.H., 1999. Degradation of phenol under meso- and thermophilic, anaerobic conditions. Anaerobe 5, 25–35.
Kelleher, B.P., Simpson, A.J., 2006. Humic substances in soils: are they really chemically distinct? Environ. Sci. Technol. 40, 4605–4611.
Le, C., Stuckey, D.C., 2016. Colorimetric measurement of carbohydrates in biological wastewater treatment systems: a critical evaluation. Water Res. 94, 280–287.
Levén, L., Schnürer, A., 2005. Effects of temperature on biological degradation of phenols, benzoates and phthalates under methanogenic conditions. Int. Biodeterior. Biodegrad. 55, 153–160.
Liu, T., Sun, L., Müller, B., Schnürer, A., 2017. Importance of inoculum source and initial community structure for biogas production from agricultural substrates. Bioresour. Technol. 245, 768–777.
Ma, H., Guo, Y., Qin, Y., Li, Y.Y., 2018. Nutrient recovery technologies integrated with energy recovery by waste biomass anaerobic digestion. Bioresour. Technol. 269, 520–531.
Marcato, C.E., Mohtar, R., Revel, J.C., Pouech, P., Hafidi, M., Guiresse, M., 2009. Impact of anaerobic digestion on organic matter quality in pig slurry. Int. Biodeterior. Biodegrad. 63, 260–266.
Möller, K., Müller, T., 2012. Effects of anaerobic digestion on digestate nutrient availability and crop growth: a review. Eng. Life Sci. 12, 242–257.
Monlau, F., Sambusiti, C., Ficara, E., Aboulkas, A., Barakat, A., Carrère, H., 2015. New opportunities for agricultural digestate valorization: current situation and perspectives. Energy Environ. Sci. 8, 2600–2621.
Pavlostathis, S.G., Giraldo-Gomez, E., 1991. Kinetics of anaerobic treatment. Water Sci. Technol. 24, 35–59.
Provenzano, M.R., Malerba, A.D., Pezzolla, D., Gigliotti, G., 2014. Chemical and spectroscopic characterization of organic matter during the anaerobic digestion and successive composting of pig slurry. Waste Manag. 34, 653–660.
Qu, H.L., Guo, X.J., Chen, Y.S., Dai, B.L., He, J., Zhu, D.W., 2017. Characterization of dissolved organic matter from effluents in a dry anaerobic digestion process using spectroscopic techniques and multivariate statistical analysis. Waste Biomass Valoriz. 8, 793–802.
Sambusiti, C., Monlau, F., Ficara, E., Musatti, A., Rollini, M., Barakat, A., et al., 2015. Comparison of various post-treatments for recovering methane from agricultural digestate. Fuel Process. Technol. 137, 359–365.
Schnürer, A., 2016. Biogas production: microbiology and technology. Adv. Biochem. Eng. Biotechnol. 156, 195–234.
Shakeri Yekta, S., Gonsior, M., Schmitt-Kopplin, P., Svensson, B.H., 2012. Characterization of dissolved organic matter in full scale continuous stirred tank biogas reactors using ultrahigh resolution mass spectrometry: a qualitative overview. Environ. Sci. Technol. 46, 12711–12719.
Shakeri Yekta, S., Hedenström, M., Stehr, J.E., Dario, M., Hertkorn, N., Björn, A., 2018. Pretreatment of anaerobic digester samples by hydrochloric acid for solution-state1H and13C NMR spectroscopic characterization of organic matter. Chemosphere 199, 201–209.
Simpson, A.J., Song, G., Smith, E., Lam, B., Novotny, E.H., Hayes, M.H.B., 2007. Unraveling the structural components of soil humin by use of solution-state nuclear magnetic resonance spectroscopy. Environ. Sci. Technol. 41, 876–883.
Simpson, A.J., McNally, D.J., Simpson, M.J., 2011. NMR spectroscopy in environmental research: from molecular interactions to global processes. Prog. Nucl. Magn. Reson. Spectrosc. 58, 97–175.
Smernik, R., Oades, J., 2000. Effect of paramagnetic cations on solid state C-13 nuclear magnetic resonance spectra of natural organic materials. Commun. Soil Sci. Plant Anal. 31, 3011–3026.
Soucémarianadin, L.N., Erhagen, B., Nilsson, M.B., Öquist, M.G., Immerzeel, P., Schleucher, J., 2017. Two dimensional NMR spectroscopy for molecular characterization of soil organic matter: application to boreal soils and litter. Org. Geochem. 113, 184–195.
Sun, L., Liu, T., Müller, B., Schnürer, A., 2016. The microbial community structure in industrial biogas plants influences the degradation rate of straw and cellulose in batch tests. Biotechnol. Biofuels 9.
Svensson, K., Kjørlaug, O., Higgins, M.J., Linjordet, R., Horn, S.J., 2018. Post-anaerobic digestion thermal hydrolysis of sewage sludge and food waste: effect on methane yields, dewaterability and solids reduction. Water Res. 132, 158–166.

Tambone, F., Adani, F., Gigliotti, G., Volpe, D., Fabbri, C., Provenzano, M.R., 2013. Organic matter characterization during the anaerobic digestion of different biomasses by means of CPMAS 13C NMR spectroscopy. Biomass Bioenergy 48, 111–120.
Trygg, J., Wold, S., 2002. Orthogonal projections to latent structures (O-PLS). J. Chemom. 16, 119–128.
Vavilin, V.A., Fernandez, B., Palatsi, J., Flotats, X., 2008. Hydrolysis kinetics in anaerobic degradation of particulate organic material: an overview. Waste Manag. 28, 939–951.
Yang, G., Zhang, P., Zhang, G., Wang, Y., Yang, A., 2015. Degradation properties of protein and carbohydrate during sludge anaerobic digestion. Bioresour. Technol. 192, 126–130.